# Wavelet-based Speckle Filtering in Ultrasound Imaging

Raiyan Abdul Baten
*Department of ECE*
*University of Rochester*
rbaten@ur.rochester.edu

Tolga F. Aktas
*Department of ECE*
*University of Rochester*
taktas@u.rochester.edu

***Abstract*—Ultrasound images suffer from speckle noises generated by interference patterns of the reflected waves received at the sensor transducer. To aid in diagnostics, it is desirable to remove speckle noise while keeping the fine details of the underlying structures intact. In this project, we explored a wavelet-based speckle filtering method that uses soft-thresholding of wavelet coefficients of a logarithmically transformed ultrasound image. The threshold is computed as $K\frac{\sigma^2}{\sigma_x}$, where $\sigma$ and $\sigma_x$ are the standard deviations of the noise and the sub-band data of the noise-free image, respectively. We compared the performance of this algorithm against the claimed baselines (2D Median and Homomorphic Weiner), as well as against a set of highly cited methods proposed in the literature. Experimental results showed that the wavelet-based filter outperformed the Median filter by more than $8.8\%$ in terms of the correlation coefficient, and more than $6.5$ dB in terms of signal-to-MSE ratio. The wavelet-based algorithm also outperformed all the comparison algorithms we tested in all the performance metrics. These results indicate good noise removal and feature preservation performance of the wavelet-based speckle-reduction filter.**

***Index Terms*—Wavelet, Speckle, Ultrasound**

## I. Introduction

Ultrasound images are degraded by an intrinsic artifact called 'Speckle noise'. This noise is generated as the reflected waves coming back from elementary scatter surfaces interfere at the sensor transducer, causing constructive and destructive interference patterns in a random manner [1]. Speckle noise significantly deteriorates the signal-to-noise ratio and contrast resolution of ultrasound images, making the discrimination of fine details difficult for diagnostic purposes. Figure 1 shows examples of such black and white interference artifacts.

Removal of speckle noise has received decades of research efforts [1]–[3]. The process is complicated by the fact that a complete removal of all speckle artifacts is not desirable—as various organs have signature speckle patterns that can aid in diagnostics. The requirement, therefore, reduces to removing the interference artifacts without hurting the fine details of the underlying structures of interest.

Rosa et al. [4] categorized the low-level image processing techniques for speckle reduction into three classes: (i) Adaptive local filters, (ii) Anisotropic diffusion filters, and (iii) Wavelet-based filters. The adaptive local filters take a moving filter window and use local statistics within the window region to filter out speckle noise. Typically, the local mean, local variance and various functions of these two metrics are used for statistical decision-making. Examples of adaptive spatial filters include variants of the 2D median filter [5]–[7], Weiner-based filters [8], Fourier and Butterworth-based filters [9], among others. Unlike these spatial filtering techniques, anisotropic diffusion filters have the ability to simultaneously eliminate noise and preserve edges. This is achieved by processing the speckled image via solving a partial differential equation [10]. Methods that are capable of even *enhancing* the edges have also been proposed using anisotropic diffusion [11]. The wavelet-based filters use space and frequency localization information of images to rid them of speckled noise. In particular, wavelet shrinkage methods such as VisuShrink [12] and BayesShrink [13] are widely popular and adopted.

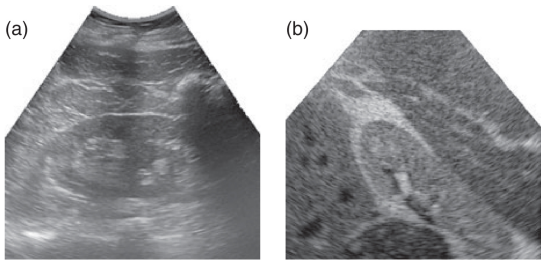


Fig. 1. Speckle noise in (a) Real and (b) Simulated ultrasound images. Adopted from [4].

In this project, we explored a wavelet-based filter proposed by Gupta et al. [14]. This method reduces speckle by modifying the wavelet-transformed sub-bands of an image using the statistical properties of the signals therein. It is based off of BayesShrink [13] and uses soft-thresholding of wavelet coefficients of a logarithmically transformed ultrasound image. Our goal is to explore how this algorithm's performance compares against the claimed baselines (2D Median and Homomorphic Weiner filters), as well as against a set of highly cited filtering methods proposed in literature.

## II. Methods

It has been shown that under certain conditions of imaging resolution and sampling, the coherent speckle noise $e$ in an image can be modelled as multiplicative noise [3]. Furthermore, it has been proposed that under certain aperture conditions, the speckle noise in a logarithmically transformed image is approximately Gaussian additive noise [15]. Thus, we have,

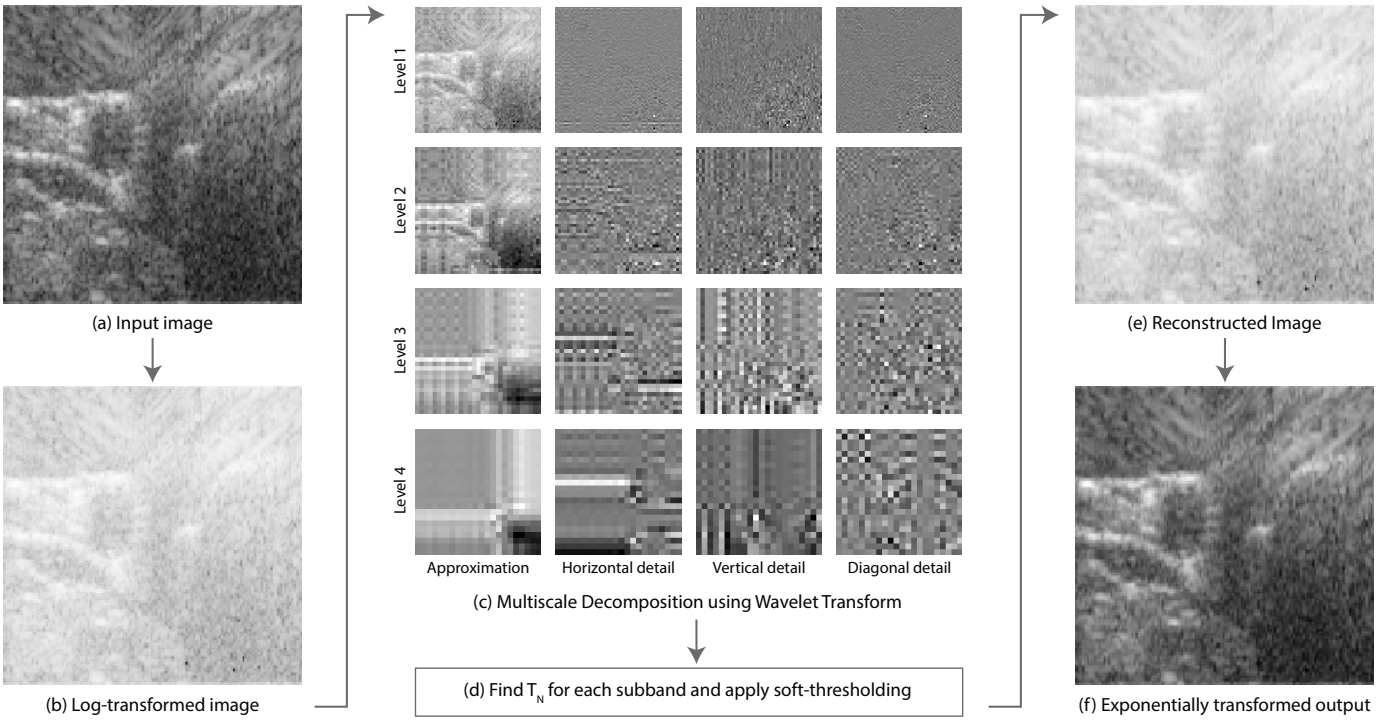


Fig. 2. Steps in the wavelet-based denoising algorithm

$$\begin{aligned} &\log I(m,n) = \log g(m,n) + \log e(m,n) \\ \implies\ &y(m,n) = x(m,n) + \eta(m,n), \end{aligned} \tag{1}$$

where $y(.), x(.)$ and $\eta(.)$ are the logarithms of the observed speckled image $I$, texture $g$, and noise $e$, respectively. The goal is to estimate the signal $\hat{I}$ from the noisy observation $I$ such that the mean squared error is minimized [14]. A visual overview of the procedure is shown in Figure 2, while the steps are shown mathematically in Algorithm 1.

We first take the logarithmic transformation of the input image $I$ (line 2 in Algorithm 1). Then, we take the discrete wavelet transform, $W$, of the log-transformed image with $J$ decomposition levels (line 3). This generates four sub-bands for each level $k$: approximation $LL_k$, horizontal detail $LH_k$, vertical detail $HL_k$, and diagonal detail $HH_k$. The noise variance $\sigma^2$ is computed from $HH_1$ (line 4). For each level, a scale parameter $K$ is computed from the level's sub-band lengths (line 6). For each detail sub-band in a level, the standard deviation $\sigma_x$ is computed (line 9). If $\sigma_x^2$ is larger than $\sigma^2$, $T_N$ is computed (line 11) and soft-thresholding is applied using $T_N$ as the threshold (line 13). If not, then $T_N$ is set to the maximum value of the sub-band, which essentially makes all the coefficients in the sub-band zero. The threshold equations are approximated by assuming a Gaussian prior and minimizing the Bayes risk,

$$T^* = \arg\min_T E[X - \eta_T(Y)]^2 \tag{2}$$

Then, the modified sub-bands are stitched together using the inverse wavelet transform $W^{-1}$ (line 15). Finally, the exponential transformation is taken to generate the output image, $\hat{I}$.

**Algorithm 1** Image Denoising Algorithm

**Input:** Noisy image $I$
**Output**: De-noised image $\hat{I}$

1: **procedure** WAVELETDENOISE($I$)
2: $I_{log} \leftarrow \log(I)$
3: $\{LL_k, LH_k, HL_k, HH_k\} \leftarrow W(I_{log})$, $k \in \{1, .., J\}$
4: $\sigma^2 \leftarrow \hat{\sigma}^2 = \left(\frac{median(|HH_1|)}{0.6745}\right)^2$
5: **for each** level $k \in \{1, .., J\}$ **do**
6: $K \leftarrow \sqrt{\log L_k}$, where size $L_k = N/2^k$
7: **for each** sub-band $I_{s,k} \in \{LH_k, HL_k, HH_k\}$ **do**
8: $\hat{\sigma}_y \leftarrow \sqrt{\frac{1}{L^2}\sum_{i,j=1}^{L} Y_{i,j}^2}$, where $Y_{i,j} \in I_{s,k}$
9: $\sigma_x \leftarrow \hat{\sigma}_x = \sqrt{max(\hat{\sigma}_y^2 - \hat{\sigma}^2, 0)}$
10: **if** $\hat{\sigma}_y^2 > \hat{\sigma}_x^2$ **and** $\hat{\sigma}_x^2 > \hat{\sigma}^2$ **then**
11: $T_N \leftarrow K\frac{\sigma^2}{\sigma_x}$
12: **else**
13: $T_N \leftarrow max(I_{s,k})$
14: $I'_{s,k} \leftarrow soft\_thresh(I_{s,k}, T_N)$
15: $I_{inv} \leftarrow W^{-1}(\{I'_{s,k} \forall s, k\})$
16: $\hat{I} \leftarrow exp(I_{inv})$
17: **return** $\hat{I}$

In this project, Raiyan implemented the wavelet-based filter, which Tolga troubleshooted. Tolga further researched and implemented the performance metric functions. Both of us participated in conducting literature review, preparing the

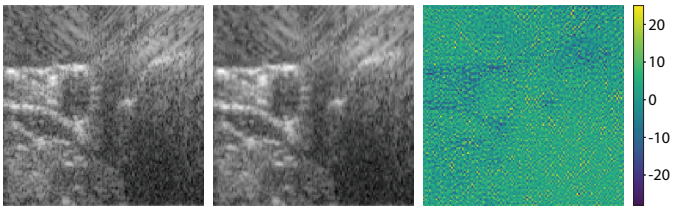


(a) Input Image (b) Wavelet-filtered Output (c) Difference (Input - Output)

Fig. 3. Input-output comparison using the wavelet-based filter.

slides and writing the report.

## III. Results

We used three test images to evaluate speckle-reduction performances. The test images were all resized to $128 \times 128$ pixels. For the wavelet transform, we employed Daubechies's least asymmetric compactly supported wavelet with eight vanishing moments at $J = 4$ scales of decomposition, as suggested by the authors [14]. Figure 3 shows the outcome of applying the wavelet-based speckle filter to one of the test images and the resulting difference image (input-output). As can be seen, the large and bright structures in the input image became even brighter in the output (blueish regions in the difference image Figure 3(c)), while the dark background mostly grew darker (greenish regions in Figure 3(c)). This gives an intuition as to how the wavelet-based filter attempts to reduce the noisy effects while preserving underlying structures.

We used three quantitative metrics to evaluate and compare between performances of different filtering methods. For speckle-filtering, the performance of a particular algorithm needs to be evaluated in terms of both the level of edge preservation and the level of noise suppression. Different metrics are required for measuring the performances in each of these criteria, and we have referred to the performance metrics such as the coefficient of correlation [16] and signal-to-MSE ratio [17] in this project, as is commonly used in literature.

For evaluating the level of noise suppression, we used two metrics: signal-to-MSE (Mean Square Error), and Pearson correlation coefficient. The former allows for a power content ratio between the signal and the noise component. The latter allows for computing a correlation between the original and the de-noised image intensities. Mathematically, we have,

$$SMSE(dB) = 10 \log_{10} \frac{\sum_{i=1}^{N \times N} I_i^2}{\sum_{i=1}^{N \times N} (\hat{I}_i - I_i)^2} \tag{3}$$

where, $I_i$ is the $i^{\text{th}}$ pixel of the input (speckled) image $I$, $\hat{I}$ refers to the de-noised output image, and $N \times N$ is the total number of pixels ($N = 128$). For the correlation coefficient metric, we have,

$$\rho = \frac{\Gamma(I - \bar{I}, \hat{I} - \bar{\hat{I}})}{\sqrt{\Gamma(I - \bar{I}, I - \bar{I}) \cdot (\hat{I} - \bar{\hat{I}}, \hat{I} - \bar{\hat{I}})}}, \tag{4}$$

where $\Gamma(x_1, x_2)$ denotes the dot product of $x_1$ and $x_2$.

TABLE I
Performance of Various Algorithms on the Test Data Images

| | Algorithm | Corr. Coeff. $\rho$ | Edge Pre. $\beta$ | Signal to MSE $SMSE$ (dB) |
|---|---|---|---|---|
| Data 1 | Wavelet | **0.98** | **0.80** | **21.59** |
| | DMF | 0.92 | 0.33 | 14.45 |
| | Weiner | 0.92 | 0.07 | 16.26 |
| | GF | 0.90 | 0.28 | 14.36 |
| | AWMF | 0.90 | 0.19 | 15.96 |
| | ARGF | 0.91 | 0.08 | 15.47 |
| | 2D Median | 0.88 | 0.02 | 12.97 |
| Data 2 | Wavelet | **0.98** | **0.78** | **24.33** |
| | DMF | 0.93 | 0.32 | 15.95 |
| | Weiner | 0.94 | 0.14 | 18.53 |
| | GF | 0.92 | 0.29 | 14.90 |
| | AWMF | 0.92 | 0.15 | 13.94 |
| | ARGF | 0.93 | 0.16 | 15.23 |
| | 2D Median | 0.90 | 0.03 | 14.50 |
| Data 3 | Wavelet | **0.99** | **0.78** | **20.43** |
| | DMF | 0.94 | 0.33 | 16.69 |
| | Weiner | 0.95 | 0.18 | 16.65 |
| | GF | 0.92 | 0.29 | 15.43 |
| | AWMF | 0.93 | 0.24 | 14.90 |
| | ARGF | 0.94 | 0.15 | 16.68 |
| | 2D Median | 0.91 | 0.03 | 13.87 |

For evaluating the level of edge preservation, we used the Pearson correlation coefficient between the high-pass Laplacian-filtered de-noised image and high-pass Laplacian-filtered original image. This allows us to measure the correlation between high frequency edge details of the original and the de-noised image. Mathematically, we have,

$$\beta = \frac{\Gamma(\Delta I - \overline{\Delta I}, \Delta \hat{I} - \overline{\Delta \hat{I}})}{\sqrt{\Gamma(\Delta I - \overline{\Delta I}, \Delta I - \overline{\Delta I}) \cdot \Gamma(\Delta \hat{I} - \overline{\Delta \hat{I}}, \Delta \hat{I} - \overline{\Delta \hat{I}})}} \tag{5}$$

where $\Delta I$ refers to the image filtered by a $3 \times 3$ Laplacian high-pass filter.

We compared the performance of the Wavelet-based filter against the claimed baselines of 2D Median Filter and Homomorphic Weiner Filter [18]. Furthermore, we chose a set of highly cited methods ($> 100$ citations) proposed in literature to compare the performances against: Directional Median Filter (DMF) [7], Geometric Filter (GF) [19], Adaptive Weighted Median Filter (AWMF) [6], and Aggressive Region Growing Filter (ARGF) [20]. The geometric filter employs an 8-hull approach while the others are adaptive local filters. The quantitative results are presented in Table I. Figure 4 provides a visual comparison among the performances of various algorithms.

It can be seen from Table I that the wavelet-based filter outperformed all of the comparison algorithms in all of the performance metrics we used (marked with bold fonts). In all of the test images, the wavelet-based filter outperformed the baseline 2D median filter by more than $8.8\%$ in terms of correlation coefficient, $2500\%$ in terms of edge preservation and more than $6.5$ dB in terms of signal-to-MSE ratio. Against the second baseline of the homomorphic Weiner filter, the

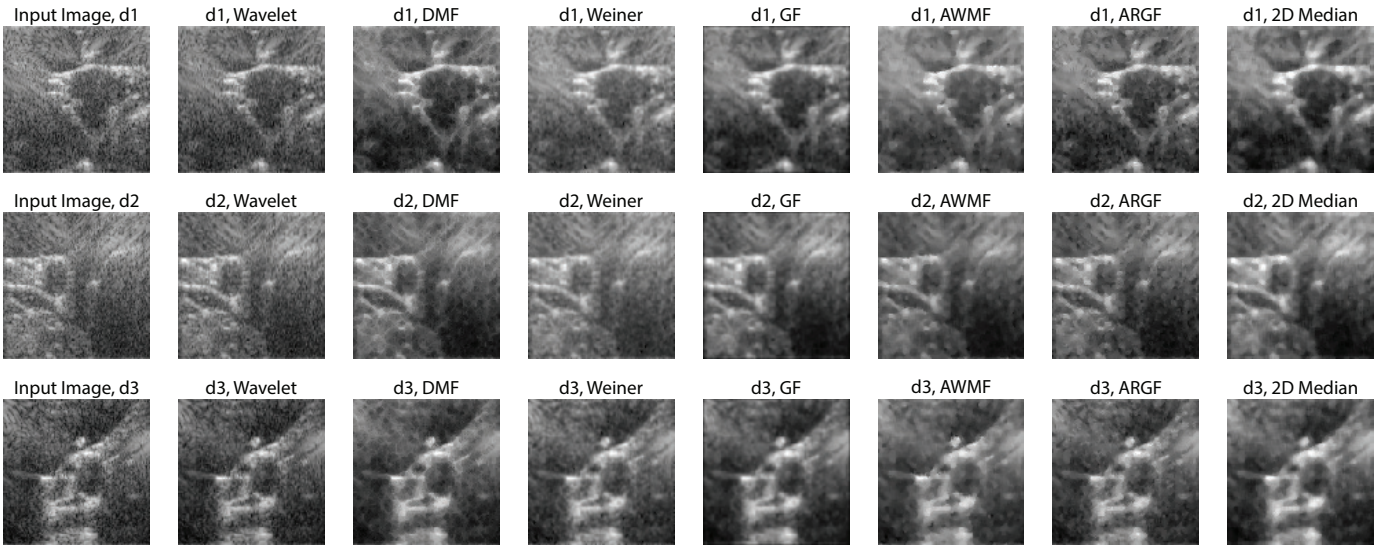


Fig. 4. Visual comparison among different algorithms on the three test images

wavelet-based algorithm once again consistently performed at least $4.2\%$ better in terms of correlation coefficient, $333\%$ better in terms of edge preservation and $3.78$ dB better in terms of signal-to-MSE ratio. Similar improvements hold against all the other comparison algorithms as well.

## IV. Discussion

Wavelet transforms provide a localized representation of the signals, allowing for space-frequency analysis. Due to this nature, wavelet-based methods are known to be useful techniques for de-noising speckled images [21]. Based on the results on the three test images, we can safely conclude that the wavelet-based statistical filtering method we explored outperforms the other 6 methods in all the performance metrics we chose. We took the 2D median and the homomorphic Wiener filters as our baselines, as suggested by the authors, and confirmed the claims of outperforming both of the baselines in both noise suppression and edge preservation metrics.

Standard noise-elimination methods often result in filtering out high-frequency features such as edges, resulting in blurring and a loss of information [14]. Our results are consistent with this phenomenon as the spatial filters (e.g., Weiner, 2D Median, ARGF) suffered in their $\beta$ values. The wavelet-based filter stood out in edge-preservation.

The proposed method exploits the multi-scale decomposition to process the speckled image at different resolutions. This provides a fine-grained mechanism for noise filtering, by applying statistically determined thresholds at different scales. Thus the method allows for differentiating between speckled noise and very-high frequency edge information. On the other hand, the comparison algorithms we tested against only analyze the input image using local statistics. Thus, the wavelet filter enjoys an upper hand in both edge preservation and noise suppression, as is evident from the quantitative results.

However, the proposed method is not without drawbacks. As the multi-scale decomposition allows for thresholding at multiple scales, the problem of de-noising reduces to finding a good choice of an adaptive thresholding method that can be applied to the various scales. The proposed algorithm is very sensitive to the selection of parameters, particularly for approximating the noise variance. The current method uses the formula $\hat{\sigma}^2 = \left(\frac{median(|Y_{ij}|)}{0.6745}\right)^2$ to approximate the noise variance. The denominator $0.6745$ is chosen as the inverse of the standard normal distribution function evaluated at $3/4$ [22]. We have observed that changing the value $0.6745$ drastically changes the performance results of the algorithm, which shows that finding a good approximation model of the noise variance is a critical factor in finding a successful thresholding function. With ample time and resources, we propose to reduce the heavy dependence of the denominator on its associated assumptions (e.g., normal distribution, evaluation at $3/4$) by approaching it as a data-driven problem. In particular, we can formulate a machine learning based scheme to rigorously test and learn the optimal parameters of the proposed algorithm from a dataset of speckled ultrasound images. This will help the algorithm to mimic the real-life characteristics of the noise variance more accurately and perhaps will lead to a more reliable speckle-reduction performance.

## V. Conclusion

In this project, we explored the use of a wavelet-based soft-thresholding approach for de-noising speckled ultrasound images. We compared our wavelet filtering method against 6 other filtering methods in the level of noise compression and edge preservation. The wavelet-based approach outperformed all in all 3 images with at least +6.5 dB improvement of Signal-to-MSE ratio, while better preserving the edge information by a large margin compared to the baseline. The multi-scale decomposition-based schemes could be extended to other

filtering and de-noising tasks due to its ability to extract finer edge information at different scales. Further investigation of the parameter learning techniques could provide better domain-specific results for de-noising tasks.

## REFERENCES


[1] S. H. C. Ortiz, T. Chiu, and M. D. Fox, "Ultrasound image enhancement: A review," *Biomedical Signal Processing and Control*, vol. 7, no. 5, pp. 419–428, 2012.

[2] J. Huang and X. Yang, "Fast reduction of speckle noise in real ultrasound images," *Signal Processing*, vol. 93, no. 4, pp. 684–694, 2013.

[3] J. W. Goodman, "Some fundamental properties of speckle," *JOSA*, vol. 66, no. 11, pp. 1145–1150, 1976.

[4] R. Rosa and F. C. Monteiro, "Performance analysis of speckle ultrasound image filtering," *Computer Methods in Biomechanics and Biomedical Engineering: Imaging & Visualization*, vol. 4, no. 3-4, pp. 193–201, 2016.

[5] D. T. Kuan, A. A. Sawchuk, T. C. Strand, and P. Chavel, "Adaptive noise smoothing filter for images with signal-dependent noise," *IEEE Transactions on Pattern Analysis & Machine Intelligence*, no. 2, pp. 165–177, 1985.

[6] T. Loupas, W. McDicken, and P. L. Allan, "An adaptive weighted median filter for speckle suppression in medical ultrasonic images," *IEEE Transactions on Circuits and Systems*, vol. 36, no. 1, pp. 129–135, 1989.

[7] R. N. Czerwinski, D. L. Jones, and W. D. O'Brien, "Ultrasound speckle reduction by directional median filtering," in *Proceedings., International Conference on Image Processing*, vol. 1. IEEE, 1995, pp. 358–361.

[8] F. Jin, P. Fieguth, L. Winger, and E. Jernigan, "Adaptive wiener filtering of noisy images and image sequences," in *Proceedings 2003 International Conference on Image Processing (Cat. No. 03CH37429)*, vol. 3. IEEE, 2003, pp. III–349.

[9] C. P. Loizou and C. S. Pattichis, "Despeckle filtering algorithms and software for ultrasound imaging," *Synthesis Lectures on Algorithms and Software in Engineering*, vol. 1, no. 1, pp. 1–166, 2008.

[10] Y. Deng, Y. Wang, and Y. Shen, "Speckle reduction of ultrasound images based on rayleigh-trimmed anisotropic diffusion filter," *Pattern Recognition Letters*, vol. 32, no. 13, pp. 1516–1525, 2011.

[11] S. Fu, Q. Ruan, W. Wang, and Y. Li, "A compound anisotropic diffusion for ultrasonic image denoising and edge enhancement," in *2005 IEEE International Symposium on Circuits and Systems*. IEEE, 2005, pp. 2779–2782.

[12] D. L. Donoho and I. M. Johnstone, "Adapting to unknown smoothness via wavelet shrinkage," *Journal of the American Statistical Sssociation*, vol. 90, no. 432, pp. 1200–1224, 1995.

[13] S. G. Chang, B. Yu, and M. Vetterli, "Adaptive wavelet thresholding for image denoising and compression," *IEEE Transactions on Image Processing*, vol. 9, no. 9, pp. 1532–1546, 2000.

[14] S. Gupta, R. Chauhan, and S. Sexana, "Wavelet-based statistical approach for speckle reduction in medical ultrasound images," *Medical and Biological Engineering and Computing*, vol. 42, no. 2, pp. 189–192, 2004.

[15] H. Arsenault and G. April, "Properties of speckle integrated with a finite aperture and logarithmically transformed," *JOSA*, vol. 66, no. 11, pp. 1160–1163, 1976.

[16] F. Sattar, L. Floreby, G. Salomonsson, and B. Lovstrom, "Image enhancement based on a nonlinear multiscale method," *IEEE Transactions on Image Processing*, vol. 6, no. 6, pp. 888–895, June 1997.

[17] A. Achim, A. Bezerianos, and P. Tsakalides, "Novel bayesian multiscale method for speckle removal in medical ultrasound images," *IEEE Transactions on Medical Imaging*, vol. 20, no. 8, pp. 772–783, Aug 2001.

[18] M. Eze and C. Osuagwu, "Evaluation of the performances of homomorphic and non-homomorphic speckle noise filtering techniques," *International Journal of Emerging Technologies in Computational and Applied Sciences (IJETCAS)*, vol. 10, p. 6, 12 2014.

[19] T. R. Crimmins, "Geometric filter for speckle reduction," *Applied optics*, vol. 24, no. 10, pp. 1438–1443, 1985.

[20] Y. Chen, R. Yin, P. Flynn, and S. Broschat, "Aggressive region growing for speckle reduction in ultrasound images," *Pattern Recognition Letters*, vol. 24, no. 4-5, pp. 677–691, 2003.

[21] H. Guo, J. E. Odegard, M. Lang, R. A. Gopinath, I. W. Selesnick, and C. S. Burrus, "Wavelet based speckle reduction with application to sar based atd/r," in *Proceedings of 1st International Conference on Image Processing*, vol. 1, Nov 1994, pp. 75–79 vol.1.

[22] R. Rosales. (2008) General statistics. https://www.ece.ubc.ca/robertor/Links_files/Files/ICCAP-2008-doc/icstat/icstat032.html. University of British Columbia.